CHANGES IN CORTICAL GRASP-RELATED ACTIVITY BEFORE AND AFTER OBJECT CONTACT

Yuke Yan[1†], Anton R. Sobinov[2,3†*], James M. Goodman[1], Elizaveta V. Okorokova[1,4], Lee E. Miller[5,6,7,8‡], Sliman J. Bensmaia[1,2,3‡]

[1]Committee on Computational Neuroscience, University of Chicago, Chicago, IL, USA
[2]Deparment of Organismal Biology and Anatomy, University of Chicago, Chicago, IL, USA
[3]Neuroscience Institute, University of Chicago, Chicago, IL, USA
[4]Department of Neurological Surgery, University of California, Davis, CA, USA
[5]Department of Neuroscience, Feinberg School of Medicine, Northwestern University, Chicago, IL, USA
[6]Department of Physical Medicine and Rehabilitation, Feinberg School of Medicine, Northwestern University, Chicago, IL, USA
[7]Department of Biomedical Engineering, McCormick School of Engineering, Northwestern University, Evanston, IL, USA
[8]Shirley Ryan AbilityLab, Chicago, IL, USA

[†]These authors contributed equally.

[‡] These authors contributed equally.

[*]Correspondence: ansobinov@uchicago.edu

Abstract

Grasping, a seemingly simple manual behavior, requires the coordinated control of dozens of joints, guided by sensory signals from muscles, tendons, and skin. As the motor cortex controls finger movement and exerted forces, the somatosensory cortex must process the barrage of proprioceptive and tactile signals that convey details about the object's shape, its local features (e.g., edges and curvature), and forces applied to it. In the present study, we aimed to understand the transformation in these sensorimotor signals at the time of contact with an object. We analyzed object-specific signals in the primary motor cortex (M1) and Brodmann's areas 3a, 1, and 2 of the somatosensory cortex of macaque monkeys. We found object information distributed throughout sensorimotor cortex, some of which was independent of contact, while most was dramatically altered by it. While all areas conveyed object information after contact, those carrying postural representations (M1, area 3a) were also informative before contact, during the hand pre-shaping epoch. Although their mappings retained some similarity between epochs, decoders built on the pre-contact epoch did not perform well on the post-contact epoch, suggesting intermixing between postural and force-related signals. After contact, individual neurons in M1 retained some information about the object, but the populational encoding of object identity weakened, reflecting perhaps, the delegation of control to subcortical structures. Unexpectedly, although it was active, area 2 was uninformative about the object before contact, despite its proprioceptive inputs. However, after contact, area 2 emerged as the most informative region of any epoch, likely reflecting its convergent proprioceptive and cutaneous input, and supporting its proposed role in haptic object perception. These results underscore the diverse activity within the sensorimotor cortex during grasping, highlighting the intricate neural processes involved in this fundamental behavior.

Introduction

When we reach to grasp an object or when one is handed to us, we pre-shape our hand to it before making contact [1–3]. We then exert just enough force to grasp, transport, and/or manipulate the object without dropping it [4]. Sensorimotor circuits control and sense the posture of the hand before contact, but they also control and sense forces after contact [5,6]. Lesion studies implicate the somatosensory and motor cortices in this circuitry, showing that lesions lead to manual deficits [7–9]. Furthermore, neural responses in motor and even somatosensory cortex have been shown to carry information about the object to be grasped before contact. During that period sensorimotor cortex encodes the posture of the hand stronger than velocity, in contrast to the arm signals, which are primarily encoded as the velocities of movement [10,11]. Additionally, there is variability in the kinematic receptive fields between areas. However, at the moment of contact, all areas of sensorimotor cortex receive a barrage of afferent information about the object. Cutaneous receptors convey information about the local features of the object and pressure on the skin [12,13], while proprioceptive – about the force exerted upon the object [14]. Considering the previous research has been focused on the period before contact is established, it is not clear how the contact affects the object-specific signals in the sensorimotor cortex, and the difference between its areas.

In the present study, we characterized the responses of neural populations in sensorimotor cortex after contact with the object was established and compared them to their pre-contact counterparts. Specifically, we measured the responses of neurons in motor (Brodmann's area 4) and somatosensory (areas 3a, 1, and 2) cortices to understand how signals about the

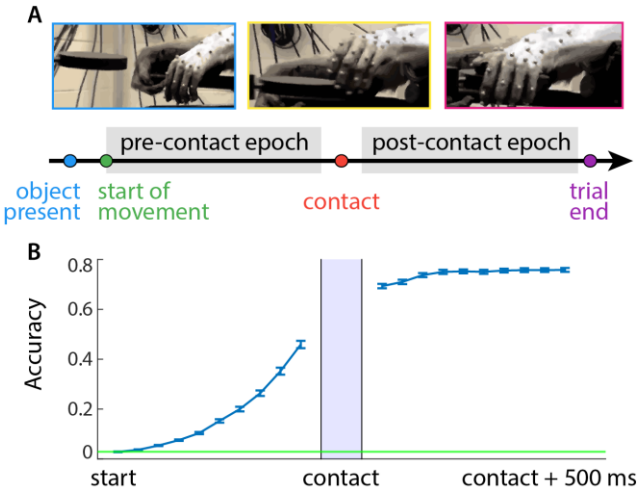

Figure 1. Behavioral task. A| Top: images of one of the trials, taken during object presentation, before, and after the contact. Bottom: Task schematic. The analysis has focused on the pre- and post-contact epochs. B| Object classification based on hand kinematics (joint angles). Classification accuracy is computed as a function of the time from the start of movement to 500 ms after contact, excluding the 100 ms period as contact is being made. Accuracy is averaged over two monkeys across all sessions. Error bars denote SEM. The chance level (2.9%) is shown in green.

object to be grasped evolve during the grasp and how they are distributed across different cortical fields. In particular, we investigated the extent to which object information is carried by neurons that receive proprioceptive input (in area 3a), neurons that receive tactile input (in area 1), and neurons that integrate these two streams of information (area 2). Neurons in primary motor cortex (M1) have been implicated in fine manual control and receive both cutaneous and musculotendonous signals [15], which strongly affect its activity during prehension [16]. Ultimately, we sought to characterize the object-related information in these different sensorimotor cortical fields, and to infer how sensory information about hand posture and interaction forces contribute to this object information.

RESULTS

We recorded the responses evoked in somatosensory and motor cortices – including Brodmann's areas 3a (34 neurons), 1 (65 neurons), 2 (36 neurons), and 4 (124 neurons) – from two rhesus macaques as they performed a grasping task (Figure 1A). In brief, a robot presented to the monkey one of 24 objects that varied in size and shape. Some of the objects were presented at different orientations, yielding 35 different grasp conditions. The monkey's task was to grasp the object with sufficient force so that the magnetic bond to the robotic arm was broken when it retracted. Each condition

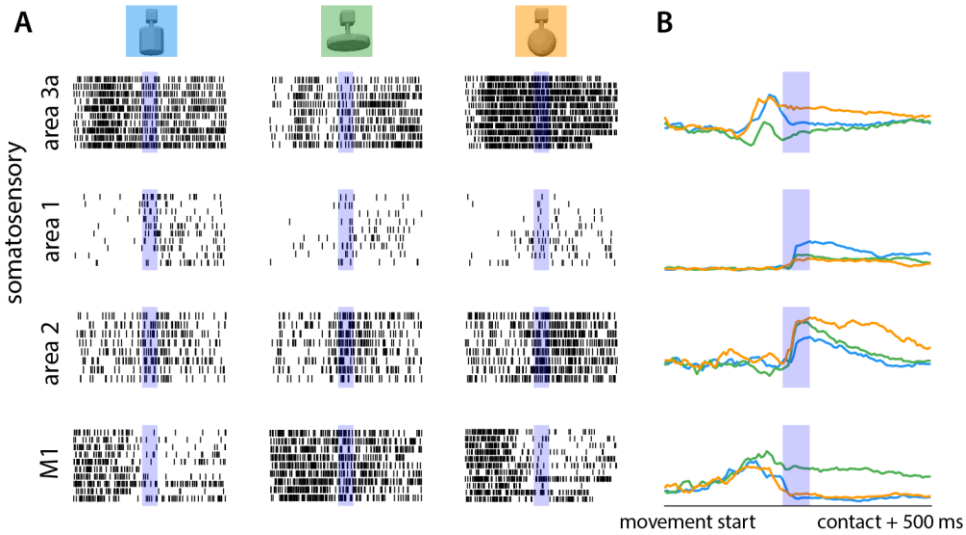

Figure 2. Activity of individual neurons in sensorimotor cortex during grasp of individual objects. A| Raster plots of one neuron each from somatosensory and motor areas as the animal grasped 3 objects over an approximately 1200-ms window centered on object contact. The shaded region shows the peri-contact epoch. **B|** Average firing rates of the neurons from A. Colors denote the objects shown in A.

was presented approximately 10 times in each experimental session. As has been previously shown, a monkey pre-shapes their hand to an object, as evidenced by the fact that object identity can be inferred from the animal's hand posture before contact (Figure 1B, [10]). While we have previously characterized the neuronal responses in this task before object contact, the objective of this study was to examine their counterparts after contact, when neural activity is driven not only by kinematics but also by contact forces. We excluded 100 ms of the peri-contact epoch from the analysis because the establishment of contact across multiple digits is not instantaneous, and different neurons will be affected differently depending on their receptive fields with strong phasic signals (Figure 2, [13]). By excluding this period, we can improve the consistency of contact-related signals in the neural response and focus on the stable states before and after contact.

Population activity in sensorimotor cortex during grasp

First, we examined the evolution of the population responses as the monkey grasped each object, beginning at movement onset through 500 ms after object contact (Figure 3A). Consistent with previous reports [17–19], we found that neurons in the different cortical areas exhibited different patterns of activity. In area 3a, activity peaked when the hand reached its maximum aperture before grasp. After contact, however,

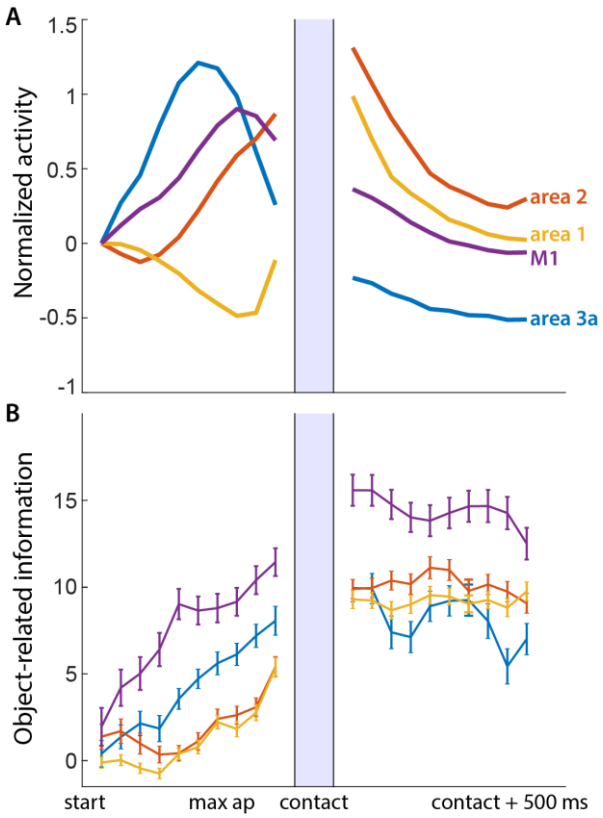

Figure 3. Time course of population activity and its informativeness in sensorimotor cortex. A| Average normalized firing rates across all neurons for each of the somatosensory areas and M1. Normalized firing rate is calculated by subtracting the raw firing rate at the start of the movement and then dividing by the standard deviation. **B|** Z-scored normalized mutual information (NMI) between activity of a neuron and the condition as a function of time.

responses in area 3a were weak even though the monkey was exerting force on the object. This weaker activity during grasp was not expected as proprioceptive neurons in these areas have been shown to encode not only kinematics but also force [5,20]. Note, however, that muscle activity also typically drops after contact [21], which may lead to a decrease in afferent input into area 3a.

In area 1, the activity was weak during the reach but surged after contact, as expected given that neurons in this cortical field have exclusively cutaneous inputs. That responses were slightly higher at movement onset than late in the pre-shaping epoch likely reflects tactile responses evoked by contact with the armrest. Area 2 had responses that reflected the combination of their counterparts in areas 3a and 1: The activity increased during the pre-shaping, as in area 3a, but rose further after contact, resembling that of area 1. This pattern of activity is consistent with the fact that area 2 receives both proprioceptive and cutaneous inputs [22–26]. In the primary motor cortex (M1), responses rose during the pre-shaping and dropped after contact. As in area 3a, the sharp drop in M1 activity is surprising, given that the monkey was exerting substantial force on the object during this epoch, although likely with muscle activity. It might reflect the control of this simpler isometric task to be passed down to subcortical structures and spinal cord [27,28].

Having established the time course of the overall amplitude of the neuronal responses in each cortical field, we examined the time course of the object-specific information over the same period (Figure 3B). To that end, we computed the normalized mutual information (NMI) [29,30] between the activity of each neuron and the identity of the grasped object in a 160 ms sliding window around each time point. We computed the Z-score by finding the number of standard deviations from the mean of a shuffled distribution to reduce the variability across neurons and emphasize variability over time. Before contact, object-related NMI averaged across neurons ramped up rapidly in area 3a, mirroring the object-specificity of hand postures. In contrast, NMI rose more slowly and to a lower level in areas 1 and 2. After contact,

area 2 was the most informative about the object, and area 3a was the least. In M1, object information ramped up rapidly prior to contact and remained high after contact. They rise earlier than object-related NMI in proprioceptive areas reflecting their causal nature.

Notably, the profiles of NMI did not match the profiles of the overall activity of each area. First, the drop in activity observed before contact in areas 3a and 4 did not result in the drop in NMIs. Second, after contact, the activity wanes in all areas, while the NMI stays approximately constant. Third, the activation peak of 3a precedes the same of M1, while NMIs peak in the opposite order. These results suggest that the activity levels in the sensorimotor cortex do not necessarily correspond to the computation of the behavior, but possibly to other mechanisms, such as attention [31].

Object-specific signals in individual cortical neurons

After establishing the time-course of the information about the object before and after contact, we wished to examine how it changed in individual neurons. To this end, we computed the mutual information between the activity of each neuron and the identity of the grasped object for 400 ms windows before and after object contact (Figure 4). High mutual information before contact would indicate primarily object-specific kinematic signals during preshaping of the hand, and after contact – both hand posture and contact forces.

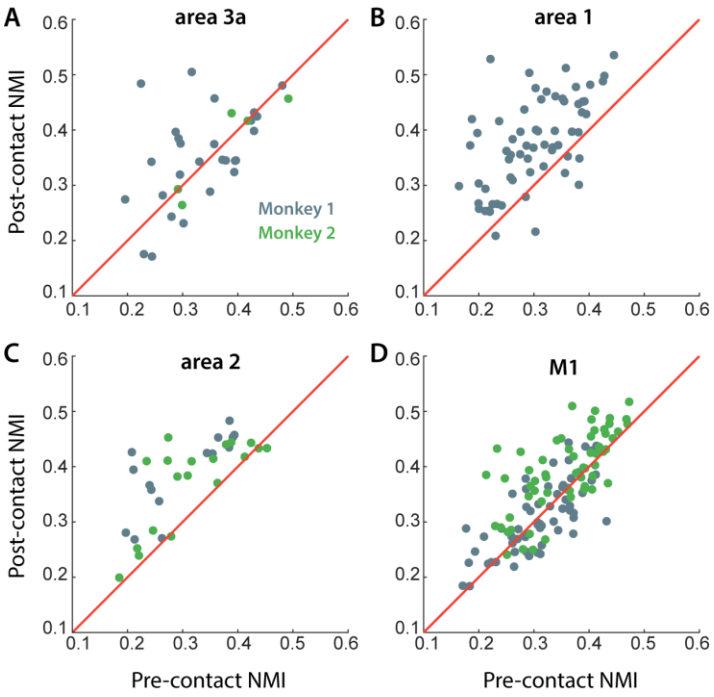

Figure 4. Object-specific signals carried by individual neurons in somatosensory areas. A| Normalized mutual information (NMI) between the activity of individual neurons in area 3a and object identity over the whole epoch. Each point denotes the informativeness of one neuron. **B, C, D**| Same as A for area 1, area 2, and M1, respectively. Red line denotes identity.

We found that most neurons in all cortical fields were informative about the object identity both before and after contact. However, in most areas (the exception being 3a, Wilcoxon signed-rank test, p=0.681, median difference=0.00067) informativeness changed at the time of contact (Figure 4A). Neurons in area 1 were far more informative after contact than before (Figure 4B, Wilcoxon signed-rank test, p=5.43e-10, median difference=0.067). Neurons in area 2 carried object-related information similar to that of area 1, in that they were more informative after contact than before (Figure 4C, Wilcoxon signed-rank test, p=1.05e-06, median difference=0.062). Notably, the proprioception-related signal before contact was less informative than the combined proprioceptive and tactile information in area 2. Throughout the sensory areas, we saw the expected pattern of high information before contact for proprioceptive areas and higher information after contact for areas with tactile inputs. In M1, neuronal responses were comparably informative before and after contact (Figure 4D, Wilcoxon signed-rank test, n=122, p=0.0012, median difference=0.011). These characteristics were consistent between the two monkeys.

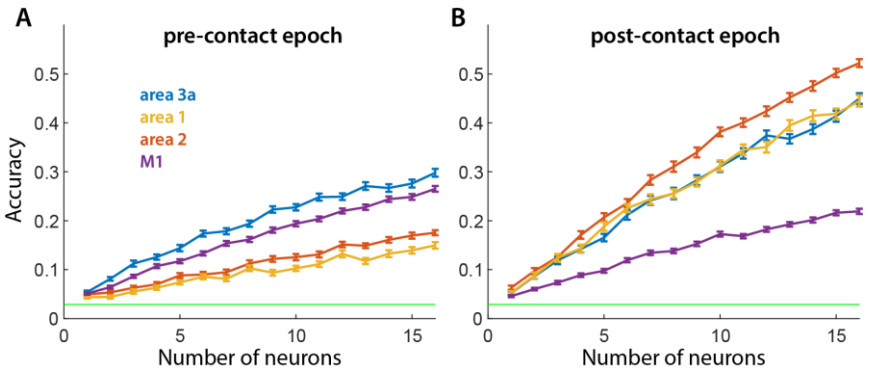

Figure 5. Classification of objects based on population responses. A| Performance of a classifier of object identity based on the responses of neurons in sensorimotor cortex before contact, as a function of sample size. **B**| Classification accuracy after contact. Green line denotes chance. Error bars denote SEM.

Object-specific signals in neural populations

The mutual information analyses gauge the degree to which individual neurons in each cortical field carry object information. To compare the populational informativeness of each area about the object, independent of the number of neurons, we analyzed the degree to which object identity could be inferred from the activity of equal numbers of random subgroups of neurons (Figure 5). Among the somatosensory areas, area 3a yielded the highest classification performance prior to contact and area 2 after contact. M1

classification accuracy was higher than somatosensory areas before contact, consistent with the previous analyses. However, after contact, populational classification accuracy from M1 was lower than that of somatosensory areas. This might suggest a highly coordinated structure of activity in M1, where each neuron is informative about the object, but with strong similarities in the object-specific signal. However, analysis of the variance structure (Supplementary Figure 1) demonstrates a similar dimensionality of M1 area to area 1 signals after contact, warranting a different explanation.

We have demonstrated that all the areas we recorded from carry object-specific information. However, the outstanding question is whether that information is encoded similarly before and after contact, i.e., to what extent it is influenced by contact forces. To assess the stability of these object-specific signals before and after contact, we repeated the classification analysis using classifiers trained on data from one epoch and tested on the other (Figure 6). We reasoned that a purely kinematic representation would be stable across epochs because hand posture immediately before contact is similar to that just after. Instead, we found that the cross-epoch classifiers (Figure 6, purple) all performed poorly, indicating that the object representations changed dramatically upon object contact.

Although the decoders did not generalize well through the contact, we hypothesized that there might be a unified representation preserved throughout the behavior. To test this, we trained a classifier on combined pre- and post-contact data and evaluated its performance for each epoch separately (Figure 6, orange). In both somatosensory areas 1 and 2, the classifier performed poorly on the pre-contact epoch, corresponding to the lack of postural information pre-contact in area 1 and suggesting a strong effect of tactile information on the proprioceptive one in area 2. Although this classifier performed better than chance in both areas 3a and M1, it still suffered a significant drop in performance (median drop in accuracy 26% and 30%, respectively), consistent with the interpretation that these two areas carry information about hand posture. The drop in the decoders' performance suggests that the signals about contact forces

are combined with the postural signals in those areas. Interestingly, the drop in performance relative to the within-epoch classifier was larger post-contact than pre-contact (8% drop vs 43% in area 3a, and 23% vs 36% in M1), suggesting that postural information is integrated with tactile post-contact, muddling the pure-postural representation. These results are further supported by joint angle decoding from the neuronal population, showing similar trends (Supplementary Figure 2). Overall, all areas hold information about the grasped object post-contact, and those representations are affected by the exertion of forces on the grasped object.

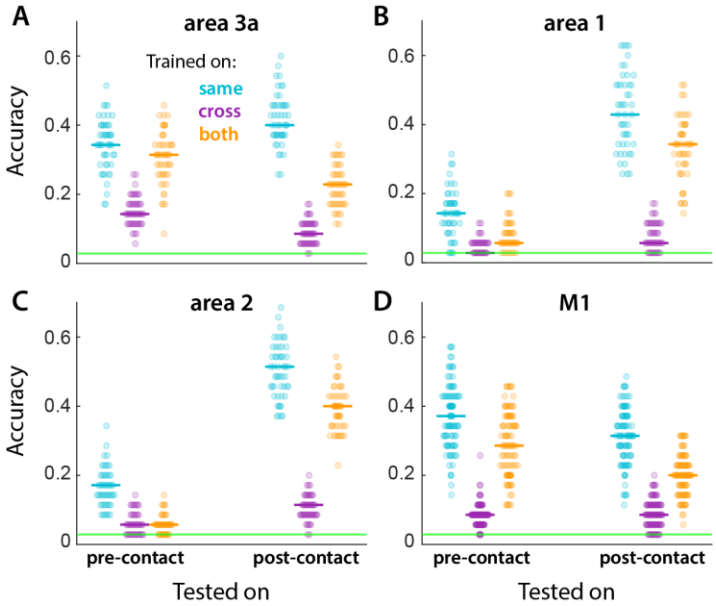

Figure 6. Stability of object-specific signals across epochs. A| Performance of classifiers of object identity based on the responses of neurons in area 3a trained and tested within the same epoch (cyan), trained in one epoch and tested in the other (purple), and trained in both epochs then tested in each (orange). The "pre-contact" vs "post-contact" column indicates the test epoch. Each point denotes the accuracy of classification based on a random allocation of training and testing data and the bold line denotes the median performance. **B, C, D|** Same as A for area 1, area 2, and M1, respectively.

Discussion

Manual dexterity is facilitated by an expansive neural network that spans large swaths of the cortex [32–34]. Different nodes within this network are thought to make different albeit overlapping contributions to hand control, so it is not surprising that contact with an object would affect the sensorimotor areas in distinct ways (cf. [17]).

In preparation for grasping, the hand pre-shapes to match the object, allowing for an efficient and effective grasp. It also allows object identity to be inferred from the shape of the hand with high accuracy before the hand touches the object [18,35]. The proprioceptive information about limb posture and movement transduced by muscle receptors (muscle spindles and Golgi tendon organs) is received by area

233 3a of the somatosensory cortex [5,22,36–40]. It is not surprising then that the activity of area 3a peaks before
234 contact, as the hand reaches its maximum aperture [10,11]. Interestingly, while the response strength peaks
235 at maximum aperture, its informativeness peaks at contact, as the hand begins to conform to the object.
236 Activity in 3a drops sharply after contact, although surprisingly, without a significant impact on the
237 informativeness of individual 3a neurons. A similar phenomenon of decreased activity during contact has
238 been previously documented in a subgroup of cortical somatosensory neurons [17,19]. Furthermore, muscle
239 activity also decreases after contact [21], which might reduce the signal coming from proprioceptive sensors.

240 Motor cortical informativeness peaks earlier than that of the proprioceptive area 3a, reflecting its causal
241 nature [19]. After contact, M1 activity declines, which conceivably drives the aforementioned decrease in
242 muscle activity. From the functional perspective, the M1's control of the hand shifts to maintaining the
243 forces in an isometric posture. The addition of the force control signal to M1 activity arguably makes it
244 even more object-specific. However, the informativeness of subpopulations of M1 neurons after contact
245 was lower than before contact (Figure 5) and lower than that of the somatosensory areas. Conceivably, it
246 is a product of the decreased activity levels in M1 after contact. The decrease in activity might reflect the
247 control of the hand motion being passed down to subcortical structures and the spinal cord. For example,
248 reticular formation has been implicated in the control of gross hand movements [28,41,42]. The spinal
249 interneurons, in turn, often exhibit sustained responses during isometric wrist tasks as opposed to a
250 phasic encoding of variables in the motor cortex [27,43]. Although the contribution of the cortex to control
251 might decrease, our results suggest that it still holds object information throughout the task.

252 While the information about the object is always present, it changes after contact, highlighting the
253 entanglement of postural and kinetic signals. If the signals were fully kinematic and unaffected by force,
254 decoders built on pre-contact epochs might be expected to perform on post-contact epochs as well as on
255 their original domain, but they do not. While these points present a different view from the suspected
256 orthogonality of postural and force signals in M1 [44,45], we cannot test it directly because the experimental

setup did not record interaction forces or electromyograms. Furthermore, it is necessary to acknowledge, that the decoders built on data combined from both epochs can extract some postural representation, which is invariant to the contact.

In stark contrast to areas 3a and 4, area 1 is nearly quiescent before contact, with weak signals that are almost completely uninformative about the object. This response pattern aligns with the fact that area 1 receives exclusively cutaneous inputs [26], suggesting that pre-contact cutaneous signals are largely uninformative about hand posture. While cutaneous signals have been shown to convey information about the posture of individual joints [46,47], our results suggest that they do not encode hand state under naturalistic conditions, where multiple joints are deflected simultaneously [11]. Area 1, however, becomes highly informative about the object after contact. Following contact, there are at least two ways in which cutaneous signals might be informative about an object in the current experimental paradigm, where the object is handed to the animal in a specific way. First, the pattern of contacts on the skin might vary across objects, which would be reflected in different patterns of activation across the neural population [26]. Second, cutaneous signals might carry information about the local features of the object – such as edge, curvature, and texture – at each point of contact. Both of these sources of cutaneous information could contribute to the performance of object decoders based on area 1 activity after contact.

Area 2 exhibits response properties that qualitatively resemble those in area 1. Indeed, the strength of the response in area 2 and informativeness about objects keep rising before the moment of contact, similar to area 1. However, area 2 responses become even more object-specific after contact, likely reflecting the convergence of cutaneous and musculotendinous signals. Area 2 is the first stage along the somatosensory neuraxis where signals from the skin and signals from the muscles and tendons are integrated [22–24,48]. In principle, then, cutaneous information about contact forces and local features at each point of contact can be combined with information about hand posture (and muscle forces) carried by musculotendinous signals to yield a signal that is more informative about object identity. Results from the

information theory and classification analyses support this hypothesis. The question remains as to why area 2 is relatively uninformative about objects before contact. One possibility is that information about hand posture inherited from area 3a is obscured by cutaneous inputs inherited from area 1. Those responses reflect the skin stretch during pre-shaping and are not informative about the object's identity. Then, the neurons in area 2 combine object-specific proprioceptive information with uninformative tactile signals, leading to low classification rates before contact. The strong effect of tactile signals on object representation is also highlighted by the inability of decoders to generalize between epochs. However, once contact is established, the cutaneous signals enhance the postural representation of the object in area 2 neurons, making them the most informative about the object's identity. This highlights the crucial role of area 2 in establishing object identity based on somatosensory cues.

CONCLUSIONS

In conclusion, each area of the sensorimotor cortex exhibits distinct patterns of activity during grasping, highlighting the complexity of the neural basis of hand control and somatosensation. Motor and proprioceptive areas are highly informative about object identity already before contact and remain so after contact, though their object representations change. This shift might reflect the musculoskeletal basis of object-related signals, which intertwine the kinetic and kinematic representations. Area 1 is uninformative about object identity before contact, indicating that whole-hand posture is poorly encoded in cutaneous neurons. In contrast, area 2 uniquely integrates these inputs and becomes highly informative after contact, consistent with its putative role in stereognosis. The weak informativeness of area 2 before contact suggests a strong entangling of cutaneous and proprioceptive signals, obscuring a purely postural representation coming from area 3a. Overall, the effects of contact on the object-related information in the areas of the sensorimotor cortex emphasize their function and anatomy.

METHODS

304 *Animals and surgery*

305 Two male rhesus macaque subjects – 6 and 15 years old, weighing 8 and 11 kg, respectively – participated
306 in this study. All animal procedures were performed in accordance with the rules and regulations of the
307 University of Chicago Animal Care and Use Committee. Monkeys received care from a full-time husbandry
308 staff, and a full-time veterinary staff monitored animals' health on a daily basis. Both monkeys were
309 implanted with a head-fixing post onto the skull. Monkey 1 was implanted with floating microelectrode
310 arrays (FMAs, Microprobes for life science, Gaithersburg, MD) and Utah electrode arrays (UEAs, Black-
311 rock Microsystems, Inc. Salt Lake City, UT). Monkey 2 was implanted twice, first with semi-chronic array
312 with electrodes of adjustable depth (Gray Matter Research, Bozeman, MT), and then with two UEAs. All
313 procedures were performed under aseptic conditions and anesthesia induced with ketamine HCl (20 mg
314 kg^{-1}, IM) and maintained with isoflurane (10–25 mg kg^{-1} per hour, inhaled).

315 *Behavioral task*

316 Monkeys were trained to grasp 35 objects varying in size, shape, and orientation. In a typical grasp trial,
317 the monkey sat in a chair with its heads fixed and arms rested on cushioned armrests. The arm of the
318 monkey remained largely immobile during the grasp. At the start of the trial, a robotic arm directly facing
319 the monkey presented an object. The monkey was trained to grasp the object and apply enough grip
320 force such that, when the robotic arm retracted, the object would be disengaged from its magnetic
321 coupling with the robot and remain in the monkey's hand. The stationarity of monkey's arm was enforced
322 by a photosensor on the armrest which ended the trial (without reward) if the arm was lifted to expose it
323 to light. For more details, refer to [10,11].

324 *Electrophysiology*

325 For monkey 1, we recorded from UEAs implanted in the pre-central and post-central gyri and FMAs
326 implanted in the posterior and anterior banks of the central sulcus. For monkey 2, we first recorded from

327 depth-adjustable electrode arrays placed over the central sulcus (first implant), then from the UEAs in the
328 pre- and post-central gyri (second implant). Offline spike sorting (Offline Sorter, Plexon, Dallas, TX) was
329 used to isolate individual units and identify spikes. Somatosensory units were classified based on
330 anatomical locations and manual functional mapping prior to recordings (see [10] for more details).

331 *Kinematics*

332 We measured hand kinematics using a marker-based motion tracking system (Vantage, VICON, Los
333 Angeles, CA). In brief, 30 photoreflective markers were placed on the back of the monkey's hand, covering
334 major joints of the hand and wrist. Ten to fourteen infrared cameras, placed around the workspace,
335 tracked the markers at 100 Hz. We then used the Vicon Nexus software (VICON, Los Angeles, CA) to
336 reconstruct the 3D position of each marker, manually labelling markers that were missing due to occlusion.
337 Then, we used a musculoskeletal model (scaled to the monkey's size) in OpenSim [49] to perform inverse
338 kinematics, which inferred the time-varying joint angles of the hand from the 3D marker positions. Joint
339 angles were smoothed with a 50-ms moving average and the angular velocities were computed from these.

340 *Parsing different trial epochs*

341 For each trial, we identified start of movement (finger and wrist position deviates from rest) and contact
342 with the object (finger and palm stop moving after conforming to the object). For monkey 1, the events
343 were labelled manually for all trials. For monkey 2, we first manually labelled a subset of the trials, then
344 trained a multi-class linear discriminant analysis classifier (LDA) using the joint angular velocities 200 ms
345 before and after each frame. We used the trained classifier to identify the key kinematic events in the
346 remaining trials. Among all sessions from monkey 2, the mean and the standard error of the model
347 deviation from left-out hand-labeled events were 16 ± 9.5 ms for start of finger movement, 21 ± 8.8 ms
348 for start of wrist movement,–25 ± 9.7 ms for palm contact with an object, and –48 ± 12.1 ms for finger
349 contact with an object. For more details, refer to [10,11].

Neural data preprocessing

After sorting, neural responses were first divided into non-overlapping 10-ms bins. For each trial, we aligned neural activity with the kinematic events identified as described above, restricting our analysis to the period from movement onset to 500 ms after first contact with the object. The pre-contact period begins at movement onset and ends 50 ms before first contact and the post-contact period begins from 50 ms after contact to 500ms after contact. We then divided each epoch of each trial into 10 equal periods, aligned these 20 timepoints across trials, and computed normalized mutual information (NMI) over a 160-ms window centered on each time point. To compensate for the fact that digits contact the object at different times, we excluded neural activity over a 100-ms window centered around first contact.

Mutual information analysis

To quantify the information about the grasped object carried by each neuron's response, we used the normalized mutual information (NMI), which was computed as follows:

First, we computed the entropy (H) of the neuron's response:

$$H\ (neuron) = -\sum_{s} P(s) * \log\ (P(s))$$

where ***s*** denotes the neuron's spike count over a specified time window (e.g., 200 ms before contact). Then we computed the condition entropy of the neuron, given each object, **o**:

$$H\ (s \mid o) = -\sum_{s,o} P(s,o) * \log\ (P(s \mid o))$$

Next, we computed the mutual information:

$$MI(s,o) = H(s) - H(s \mid o)$$

The mutual information was then normalized by the neuron's overall entropy:

370 $$NMI = \frac{MI\ (neuron, object)}{H(neuron)}$$

371 The resulting metric, NMI, ranges from 0 to 1. We did not include $H(object)$ in the normalization because
372 this term depends only on the number of trials for each object and was therefore constant for all neurons.
373 In Figure 3, we standardized the NMI with respect to a chance-level NMI, calculated by randomly shuffling
374 the spike counts at the start of the movement with respect to the object identity. We then calculated the
375 mean NMI with the shuffled data and repeated the process 100 times to generate a distribution of mean
376 NMIs. Raw mean NMI values were then expressed in terms of standard deviations from the mean (z-
377 scores) chance-level NMI.

378 *Classification*

379 To investigate the object information carried by populations of neurons, we used a classification analysis.
380 In brief, we pooled trials across sessions and calculated the spike count for a 400-ms pre-contact window
381 and one after contact. Each window excluded a 100-ms buffer zone around contact, as described above.
382 In preliminary analyses, we found that a 400 ms window provided the best classification accuracy across
383 cortical fields. We then used an object-level leave-one-out classification paradigm: For each object, we
384 randomly selected a test trial and used the remaining trials as training trials. We then trained a linear
385 discriminant analysis classifier (LDA) on the training trials and calculated the classification accuracy on the
386 test trials. For each cortical region, we repeated this process 100 times and calculated the mean accuracy.
387 To assess the effect of population size, we randomly selected a subset of neurons in each iteration and
388 computed the mean accuracy as a function of sample size.

389 We also performed an across-epoch classification analysis to understand the stability of object signals
390 before and after contact. To this end, we used the same pre-and post-contact window and leave-one-out
391 paradigm, but tested classifiers trained with data from one window on data from the other. We also
392 trained the LDA classifier on the combined training data from both epochs and tested it on either epoch,

using leave-one-out cross-validation ("both" classifier in Figure 6 A-D).

AUTHOR CONTRIBUTIONS

YY, ARS, and SJB designed the study. JMG and EVO performed the experiments. YY and ARS performed the analysis. ARS, LEM, and SJB supervised the work at different stages. YY, ARS, and LEM wrote the manuscript with input from all authors.

COMPETING INTERESTS

ARS served as a consultant for Google DeepMind at the time of the study. The authors declare no competing interests.

References

1. Jeannerod, M. *The Neural and Behavioural Organization of Goal-Directed Movements.* xii, 283 (Clarendon Press/Oxford University Press, New York, NY, US, 1988).
2. Santello, M., Flanders, M. & Soechting, J. F. Patterns of hand motion during grasping and the influence of sensory guidance. *J. Neurosci.* **22**, 1426–1435 (2002).
3. Yan, Y., Goodman, J. M., Moore, D. D., Solla, S. A. & Bensmaia, S. J. Unexpected complexity of everyday manual behaviors. *Nat. Commun.* **11**, 3564 (2020).
4. Jenmalm, P. & Johansson, R. S. Visual and Somatosensory Information about Object Shape Control Manipulative Fingertip Forces. *J. Neurosci.* **17**, 4486–4499 (1997).
5. Prud'homme, M. J. & Kalaska, J. F. Proprioceptive activity in primate primary somatosensory cortex during active arm reaching movements. *J. Neurophysiol.* **72**, 2280–2301 (1994).
6. Hepp-Reymond, M.-C., Kirkpatrick-Tanner, M., Gabernet, L., Qi, H.-X. & Weber, B. Context-dependent force coding in motor and premotor cortical areas. *Exp. Brain Res.* **128**, 123–133 (1999).
7. Glees, P. & Cole, J. Recovery of skilled motor functions after small repeated lesions of motor cortex in macaque. *J. Neurophysiol.* **13**, 137–148 (1950).
8. Friel, K. M. & Nudo, R. J. Recovery of motor function after focal cortical injury in primates: compensatory movement patterns used during rehabilitative training. *Somatosens. Mot. Res.* **15**, 173–189 (1998).
9. Isa, T. Dexterous Hand Movements and Their Recovery After Central Nervous System Injury. *Annu. Rev. Neurosci.* **42**, 315–335 (2019).
10. Goodman, J. M. *et al.* Postural Representations of the Hand in the Primate Sensorimotor Cortex. *Neuron* **104**, 1000-1009.e7 (2019).
11. Okorokova, E. V., Goodman, J. M., Hatsopoulos, N. G. & Bensmaia, S. J. Decoding hand kinematics from population responses in sensorimotor cortex during grasping. *J. Neural Eng.* **17**, 046035 (2020).

425 12. Johansson, R. S. & Flanagan, J. R. Coding and use of tactile signals from the fingertips in object
426 manipulation tasks. *Nat. Rev. Neurosci.* **10**, 345–359 (2009).
427 13. Callier, T., Suresh, A. K. & Bensmaia, S. J. Neural Coding of Contact Events in Somatosensory Cortex.
428 *Cereb. Cortex* **29**, 4613–4627 (2019).
429 14. Prochazka, A. & Ellaway, P. Sensory systems in the control of movement. *Compr. Physiol.* **2**, 2615–
430 2627 (2012).
431 15. Strick, P. L. & Preston, J. B. Two representations of the hand in area 4 of a primate. II.
432 Somatosensory input organization. *J. Neurophysiol.* **48**, 150–159 (1982).
433 16. Suresh, A. K. *et al.* Neural population dynamics in motor cortex are different for reach and grasp.
434 *eLife* **9**, e58848 (2020).
435 17. Debowy, D. J., Ghosh, S., Gardner, E. P. & Ro, J. Y. Comparison of neuronal firing rates in
436 somatosensory and posterior parietal cortex during prehension. *Exp. Brain Res.* **137**, 269–291
437 (2001).
438 18. Gardner, E. P. *et al.* Neurophysiology of Prehension. I. Posterior Parietal Cortex and Object-Oriented
439 Hand Behaviors. *J. Neurophysiol.* **97**, 387–406 (2007).
440 19. Gardner, E. P., Ro, J. Y., Babu, K. S. & Ghosh, S. Neurophysiology of Prehension. II. Response
441 Diversity in Primary Somatosensory (S-I) and Motor (M-I) Cortices. *J. Neurophysiol.* **97**, 1656–1670
442 (2007).
443 20. Chowdhury, R. H., Glaser, J. I. & Miller, L. E. Area 2 of primary somatosensory cortex encodes
444 kinematics of the whole arm. *eLife* **9**, e48198 (2020).
445 21. Brochier, T., Spinks, R. L., Umilta, M. A. & Lemon, R. N. Patterns of muscle activity underlying object-
446 specific grasp by the Macaque monkey. *J. Neurophysiol.* **92**, 1770–1782 (2004).

22. Iwamura, Y., Tanaka, M., Sakamoto, M. & Hikosaka, O. Rostrocaudal gradients in the neuronal receptive field complexity in the finger region of the alert monkey's postcentral gyrus. *Exp. Brain Res.* **92**, (1993).

23. Taoka, M., Toda, T., Iriki, A., Tanaka, M. & Iwamura, Y. Bilateral receptive field neurons in the hindlimb region of the postcentral somatosensory cortex in awake macaque monkeys. *Exp. Brain Res.* **134**, 139–146 (2000).

24. Seelke, A. M. H. *et al.* Topographic Maps within Brodmann's Area 5 of Macaque Monkeys. *Cereb. Cortex* **22**, 1834–1850 (2012).

25. Kim, S. S., Gomez-Ramirez, M., Thakur, P. H. & Hsiao, S. S. Multimodal Interactions between Proprioceptive and Cutaneous Signals in Primary Somatosensory Cortex. *Neuron* **86**, 555–566 (2015).

26. Delhaye, B. P., Long, K. H. & Bensmaia, S. J. Neural Basis of Touch and Proprioception in Primate Cortex. in *Comprehensive Physiology* (ed. Terjung, R.) 1575–1602 (Wiley, 2018). doi:10.1002/cphy.c170033.

27. Fetz, E. E., Perlmutter, S. I., Prut, Y., Seki, K. & Votaw, S. Roles of primate spinal interneurons in preparation and execution of voluntary hand movement. *Brain Res. Rev.* **40**, 53–65 (2002).

28. Baker, S. N. The primate reticulospinal tract, hand function and functional recovery. *J. Physiol.* **589**, 5603–5612 (2011).

29. Shannon, C. E. A mathematical theory of communication. *Bell Syst. Tech. J.* **27**, 379–423 (1948).

30. Timme, N. M. & Lapish, C. A Tutorial for Information Theory in Neuroscience. *eNeuro* **5**, ENEURO.0052-18.2018 (2018).

31. Johansen-Berg, H. & Matthews, P. Attention to movement modulates activity in sensori-motor areas, including primary motor cortex. *Exp. Brain Res.* **142**, 13–24 (2002).

470 32. Baldwin, M. K. L., Cooke, D. F., Goldring, A. B. & Krubitzer, L. Representations of fine digit
471 movements in posterior and anterior parietal cortex revealed using long-train intracortical
472 microstimulation in macaque monkeys. *Cereb. Cortex* **28**, 4244–4263 (2018).
473 33. Goldring, A. B. & Krubitzer, L. A. Chapter 26 - Evolution of Parietal Cortex in Mammals: From
474 Manipulation to Tool Use. in *Evolutionary Neuroscience (Second Edition)* (ed. Kaas, J. H.) 627–656
475 (Academic Press, London, 2020).
476 34. Sobinov, A. R. & Bensmaia, S. J. The neural mechanisms of manual dexterity. *Nat. Rev. Neurosci.* **22**,
477 741–757 (2021).
478 35. Grafton, S. T. The cognitive neuroscience of prehension: Recent developments. *Exp. Brain Res.* **204**,
479 475–491 (2010).
480 36. Krubitzer, L. & Kaas, J. The organization and connections of somatosensory cortex in marmosets. *J.*
481 *Neurosci.* **10**, 952–974 (1990).
482 37. Kaas, J. H. The functional organization of somatosensory cortex in primates. *Ann. Anat. - Anat. Anz.*
483 **175**, 509–518 (1993).
484 38. Krubitzer, L., Huffman, K. J., Disbrow, E. & Recanzone, G. Organization of area 3a in macaque
485 monkeys: Contributions to the cortical phenotype. *J. Comp. Neurol.* **471**, 97–111 (2004).
486 39. London, B. M., Jordan, L. R., Jackson, C. R. & Miller, L. E. Electrical Stimulation of the Proprioceptive
487 Cortex (Area 3a) Used to Instruct a Behaving Monkey. *IEEE Trans. Neural Syst. Rehabil. Eng.* **16**, 32–
488 36 (2008).
489 40. Schaffelhofer, S., Agudelo-Toro, A. & Scherberger, H. Decoding a Wide Range of Hand
490 Configurations from Macaque Motor, Premotor, and Parietal Cortices. *J. Neurosci.* **35**, 1068–1081
491 (2015).
492 41. Honeycutt, C. F., Kharouta, M. & Perreault, E. J. Evidence for reticulospinal contributions to
493 coordinated finger movements in humans. *J. Neurophysiol.* **110**, 1476–1483 (2013).

42. Baker, S. N. & Perez, M. A. Reticulospinal Contributions to Gross Hand Function after Human Spinal Cord Injury. *J. Neurosci.* **37**, 9778–9784 (2017).

43. Shalit, U., Zinger, N., Joshua, M. & Prut, Y. Descending Systems Translate Transient Cortical Commands into a Sustained Muscle Activation Signal. *Cereb. Cortex* **22**, 1904–1914 (2012).

44. Intveld, R. W., Dann, B., Michaels, J. A. & Scherberger, H. Neural coding of intended and executed grasp force in macaque areas AIP, F5, and M1. *Sci. Rep.* **8**, 17985 (2018).

45. Rastogi, A. *et al.* The Neural Representation of Force across Grasp Types in Motor Cortex of Humans with Tetraplegia. *eNeuro* **8**, (2021).

46. Edin, B. B. & Abbs, J. H. Finger movement responses of cutaneous mechanoreceptors in the dorsal skin of the human hand. *J. Neurophysiol.* **65**, 657–670 (1991).

47. Edin, B. B. & Johansson, N. Skin strain patterns provide kinaesthetic information to the human central nervous system. *J. Physiol.* **487**, 243–251 (1995).

48. Hyvärinen, J. & Poranen, A. Receptive field integration and submodality convergence in the hand area of the post-central gyrus of the alert monkey. *J. Physiol.* **283**, 539–556 (1978).

49. Seth, A. *et al.* OpenSim: Simulating musculoskeletal dynamics and neuromuscular control to study human and animal movement. *PLOS Comput. Biol.* **14**, e1006223 (2018).

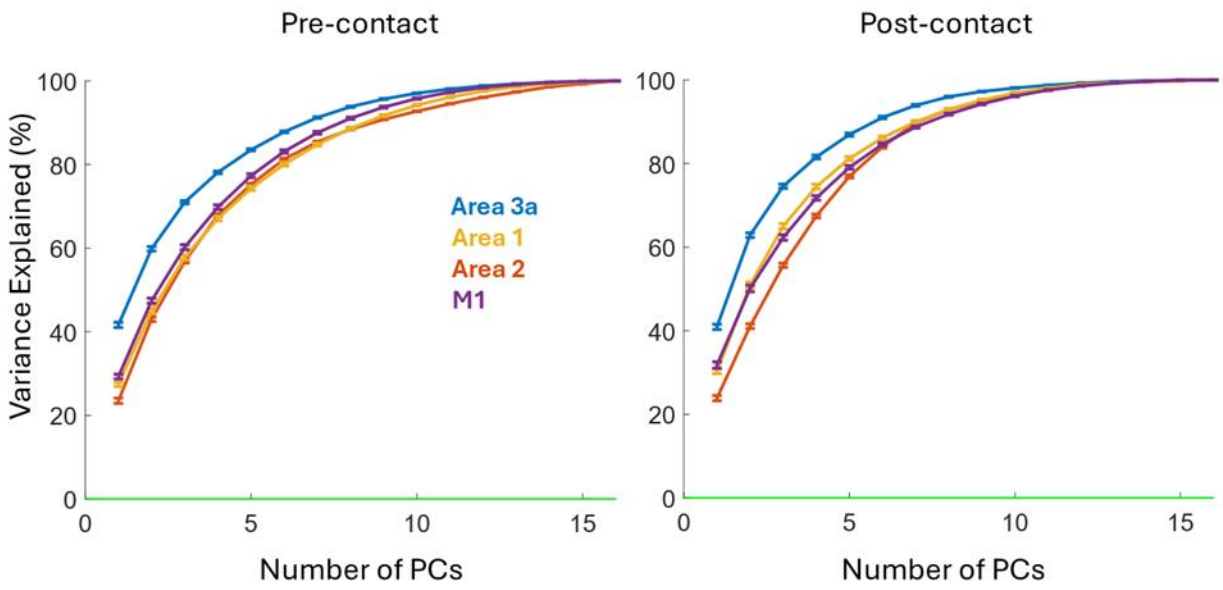

Supplementary Figure 1. Cumulative variance explained by PCA of each area. A| Cumulative scree plot for area 3a, 2, 1 and M1 before contact. PCA was performed on the spike count data pre-contact, and we record the cumulative variance explained as a function of the number of PCs. For areas with more than 16 neurons, we randomly sample 16 neurons, perform PCA, and repeat this process for 100 trials. Error bar denotes SEM. B| Cumulative scree plot after contact.

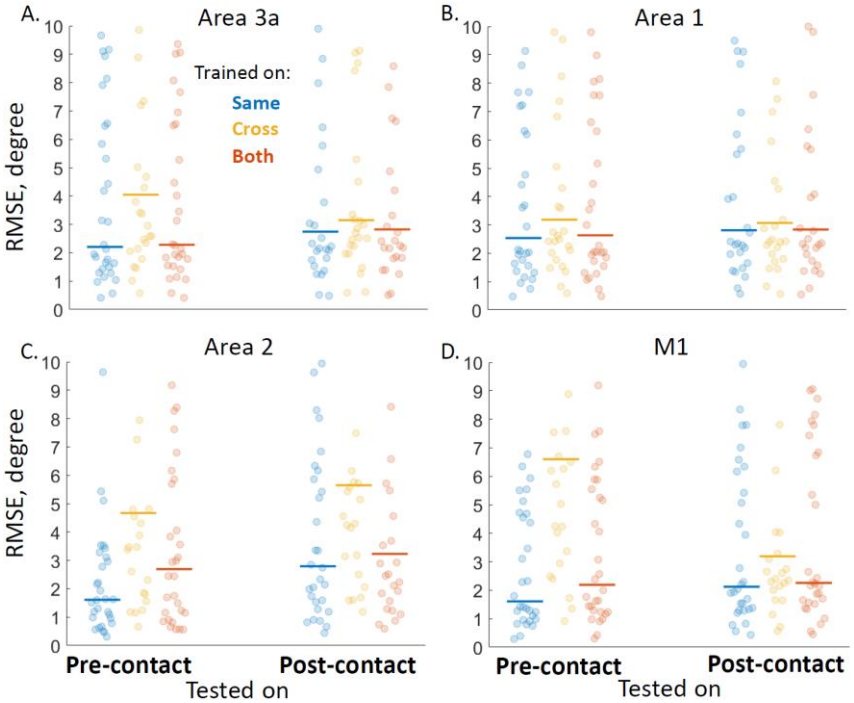

Supplementary Figure 2. Stability of kinematic signal across epochs. A| Joint angle decoding performance using the spike counts of neurons from area 3a within a 200 ms window pre-contact (left) and post-contact (right). Each dot corresponds to one of 30 joint angles, and y-axis shows the root-mean-square error (RMSE) in degrees. B| Same as A for area 1. C| Same as A for area 2. D| Same as A for M1.

To directly investigate the similarity of the postural signal before and after contact, we decoded the hand joint angles from the pre-contact and post-contact neural responses. We found that joint angles can be predicted – within a few degree's precision – from the neuronal spike counts. Marginally higher performance of the cross decoders in area 3a suggests that its representation is more consistent than M1's. Area 2's postural representations may be mixed with other signals and tend to vary more pre-contact and post-contact.